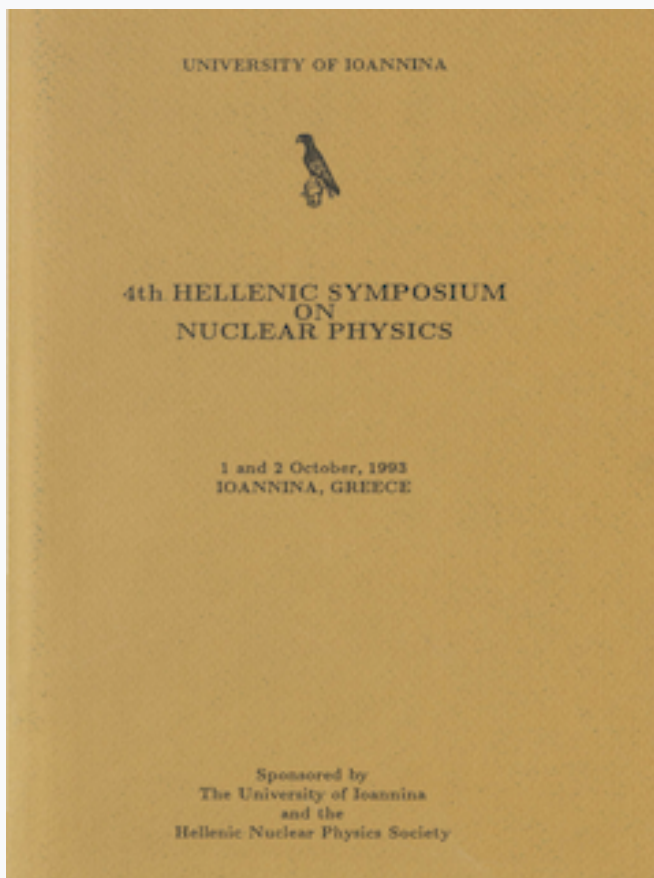


HNPS Advances in Nuclear Physics

Vol 4 (1993)

HNPS1993



Phenomenological nuclear density distributions

G. A. Lalazissis, C. P. Panos

doi: [10.12681/hnps.2877](https://doi.org/10.12681/hnps.2877)

To cite this article:

Lalazissis, G. A., & Panos, C. P. (2020). Phenomenological nuclear density distributions. *HNPS Advances in Nuclear Physics*, 4, 85–98. <https://doi.org/10.12681/hnps.2877>

Phenomenological nuclear density distributions

G. A. Lalazissis C. P. Panos
Department of Theoretical Physics
Aristotle University of Thessaloniki
GR-54006 Thessaloniki, GREECE

Abstract

A recently proposed semiphenomenological density distribution for neutrons and protons in nuclei is discussed. This density was derived using the separation energies of the last neutron or proton. A comparison is made with the symmetrised Fermi density distribution with parameters determined by fitting electron scattering experimental data and with a Fermi density with parameters coming from a recent analysis of pionic atoms. Theoretical expressions for rms radii for neutron, proton and matter distributions are proposed, which give the average trend of the variation of these quantities as functions of N , Z and A respectively. To facilitate the use of the new density all the parameters needed in a practical application are tabulated for a series of nuclei. Some applications of the new density are also discussed.

1 Introduction

Through the years a lot of information has been obtained for the nuclear charge densities by means of electron and muon scattering, nuclear reactions, mesonic atoms e.t.c. and sophisticated methods have been developed for the theoretical calculation of these densities. In addition, theoretical calculations

of the neutron and proton densities have also been performed due to the importance of these quantities in our understanding of nuclear properties. Though the theoretical models developed so far are very good, they have reached, however, a degree of complexity. Therefore, in phenomenological studies the use of phenomenological density distributions is still attractive due to their simplicity.

The most popular (for nuclei with $A \geq 18$) phenomenological density distribution is the Fermi distribution and its variants. On the other hand variants of the Gaussian distribution have been widely used mainly for light systems. The parameters of these densities are usually determined by fitting the electron and muon scattering data. From the charge density distribution derived in this way one obtains, using a process not always easy or direct, the point proton distribution, which sometimes is taken to be equal to the neutron or nucleon density distributions. A good representative of the Fermi type densities is the symmetrized Fermi distribution [1,2].

The aim of the present paper is to assess a rather recently proposed semiphenomenological nuclear density distribution for protons and neutrons separately, namely the density of Gambhir and Patil $\rho_{GP}(\mathbf{r})$ [3,4]. The interesting point is that the separation energies of the last proton or neutron are used as the only input for the determination of the parameters of this density. A comparison is made with the symmetrized Fermi density distribution $\rho_{SF}(\mathbf{r})$ with parameters coming from fitting to electron scattering experimental data and to neutron Fermi distributions obtained from pionic atoms.

In section 2 the densities $\rho_{SF}(\mathbf{r})$ and $\rho_{GP}(\mathbf{r})$ are briefly described and in section 3 numerical results are reported and certain comments are made.

2 Phenomenological density distributions

In this section we describe briefly two phenomenological densities which have certain interesting features compared with other densities used over the years in nuclear physics: First the symmetrized Fermi density distribution $\rho_{SF}(\mathbf{r})$ or the so-called universal nuclear charge density distribution [1,2] and second the density of Gambhir and Patil [3,4] $\rho_{GP}(\mathbf{r})$.

The density $\rho_{SF}(r)$ has the form:

$$\begin{aligned}\rho_{SF} &= \rho_0 \frac{\sinh(R/a)}{\cosh(r/a) + \cosh(R/a)} \\ &= \rho_0 \left(\left[1 + \exp\left(\frac{r-R}{a}\right) \right]^{-1} + \left[1 + \exp\left(\frac{-r-R}{a}\right) \right]^{-1} - 1 \right)\end{aligned}\quad (1)$$

with

$$\rho_0 = \frac{3}{4\pi R^3} \left[1 + \left(\frac{\pi a}{R} \right)^2 \right]^{-1} \quad (2)$$

The form factor of this density is very similar to that which has been recently studied in [5] for the nuclear case as well as in an analysis of Λ and Ξ hyper-nuclei [6,7]. It offers the possibility to analyze experimental form factors in the framework of the same (in other words, universal) density distribution. It has some worth mentioning features and advantages. It has zero slope at the origin, contrary to the regular Fermi distribution and therefore it is expected to be also suitable for light nuclei. Indeed, for light systems, the behaviour of $\rho_{SF}(r)$ inside the nucleus is similar to the Gaussian one, while at large distances ($r \gg R$) it shows a realistic exponential behaviour. For the medium and heavy nuclei practically it coincides with the Fermi distribution. In addition the r.m.s. radius is not a transcendental function of the radius R and the following expression is exact:

$$\langle r^2 \rangle^{1/2} = R \sqrt{\frac{3}{5}} \sqrt{1 + \frac{7}{3} \left(\frac{\pi a}{R} \right)^2} \quad (3)$$

while in the case of the Fermi distribution the above expression holds approximately, provided that $\exp(-r/a) \ll 1$, that is apart from light nuclei. Another feature of this density is that its form factor can be calculated analytically [2].

A rather recently proposed semi-phenomenological density distribution for $\rho_n(r)$, $\rho_p(r)$ [3] is the density of Gambhir and Patil $\rho_{GP}(r) = \rho_i(r)$ ($i = n$ or p for neutrons or protons respectively) which has the form:

$$\rho_i(r) = \frac{\rho_i}{1 + \beta_i \left[1 + \left(\frac{r}{R+a_i} \right)^2 \right]^{\alpha_i} \left[e^{\frac{(r-R)}{a_i}} + e^{\frac{-(r+R)}{a_i}} \right]}} \quad (4)$$

where R is a measure of the size of the nucleus and a_i and α_i are given in

terms of the separation energy E_i of the last particle (neutron or proton) by the equations:

$$a_i = \frac{\hbar}{2\sqrt{2mE_i}} \quad \alpha_i = \frac{q}{\hbar} \sqrt{\frac{m}{2E_i}} + 1 \quad (5)$$

where $q=0$ for neutrons and $q=Z-1$ for protons. The above $\rho_i(r)$ has two important features: 1) Its central behaviour is dictated by the fact that it has a vanishing slope for $r=0$. 2) It shows the correct asymptotic behaviour of the density of the particles in a nucleus. In order to identify R with the half-density radius, β_i is taken to be

$$\beta_i = [1 + (\frac{R}{R + a_i})^2]^{-\alpha_i} \quad (6)$$

The unknown parameters are ρ_n , ρ_p and R . Two of these (R and ρ_p) are determined from the normalization of ρ_n and ρ_p to N and Z respectively, while ρ_n is taken to be the same for all nuclei, namely: $\rho_n \approx 0.09/fm^3$ which gives the observed rms radius for the charge density in ^{208}Pb . Approximate analytic expressions were found for the normalization integrals and the integration for the r.m.s. radius [3], which have the form:

$$4\pi \int \rho_i(r)r^2 dr \simeq \frac{4\pi R^3}{3} \rho_i(1 + x_i^2) \quad (7)$$

$$\langle r_i^2 \rangle \simeq R^2(0.6 + 1.4x_i^2) \quad (8)$$

where

$$x_i = \frac{\pi}{z_i \left[\frac{R}{R+a_i} + \frac{2\alpha_i R^2}{(R+a_i)^2 + R^2} \right]} \quad (9)$$

3 Numerical results and comments

The calculations of Gambhir and Patil were carried out for a set of 13 nuclei. Their predictions are shown in table 1 of [3]. We repeated the calculation for a larger set of nuclei to cover the periodic table uniformly as much as possible. To facilitate the use of $\rho_{GP}(r)$, we tabulate in table 1 all the necessary

parameters which are needed in a practical application. Thus one can use directly the form of equation (4).

In a second paper [4] Gambhir and Patil removed the approximation $\rho_n \approx 0.090/fm^3$. In order to identify R with the half-density radius they take β_i to be $\beta_i = 2^{-\alpha_i}$. The unknown parameters are ρ_n, ρ_p and R. The radius R is determined by requiring that the r.m.s. radius R_p for the proton density predicted by (4) should agree with the one obtained from the experimental r.m.s. charge density radius R_c by using $R_p \approx (R_c^2 - 0.6)^{1/2}$, where 0.6 is the small correction due to the finite sizes of the proton and the neutron. The parameter ρ_n is determined from the normalization $4\pi \int \rho_n(r)r^2 dr = N$ and ρ_p from the normalization $4\pi \int \rho_p(r)r^2 dr = Z$. Again we repeated the calculation of Gambhir and Patil for a larger set of nuclei and the results for the neutron densities are shown in table 2. It is noted that in this case the relations (7) and (8) also hold but x_i is given by the following expression:

$$x_i = \frac{\pi a_i}{R + a_i \alpha_i}$$

The new density can find certain applications which are discussed below. In [8] expressions for $\langle r^2 \rangle_n$ and $\langle r^2 \rangle_p$ are derived from $\rho_{GP}(r)$ and from these the following approximate expressions can be obtained :

$$\langle r^2 \rangle_n^{1/2} = 1.147N^{1/3} + 0.698N^{-1/3} \quad \langle r^2 \rangle_p^{1/2} = 1.270Z^{1/3} + 0.175Z^{-1/3} \quad (10)$$

while from [9] the following expression for the matter rms radius may also be derived:

$$\langle r^2 \rangle_m^{1/2} = 0.956A^{1/3} + 0.572A^{-1/3} \quad (11)$$

The expressions for m.s radii were used [8] as an input for the determination of $\hbar\omega$ for neutrons and protons separately.

$$\hbar\omega_n = 34.1N^{-1/3} - 36.0N^{-1} \quad \hbar\omega_p = 27.9Z^{-1/3} - 3.2Z^{-1} \quad (12)$$

In addition in [9] the following expression for $\hbar\omega_N$ (for nucleons) was derived:

$$\hbar\omega_N(A) = 39.0A^{-1/3} - 36.8A^{-1} \quad (13)$$

In order to see the average trend of the variation of $\langle r^2 \rangle_n^{1/2}$, $\langle r^2 \rangle_p^{1/2}$ and $\langle r^2 \rangle_m^{1/2}$ with N,Z and A respectively we make a schematic plot (figure

Nucleus	R	a_n	a_p	α_p	β_n	β_p	ρ_p
¹⁶ O	2.489	0.575	0.654	1.221	0.603	0.552	0.0861
¹⁹ F	2.608	0.705	0.806	1.311	0.617	0.547	0.0777
²³ Na	2.860	0.646	0.768	1.370	0.600	0.516	0.0784
²⁴ Mg	2.927	0.560	0.666	1.353	0.587	0.502	0.0859
²⁷ Al	3.050	0.630	0.792	1.458	0.593	0.490	0.0782
²⁸ Si	3.111	0.549	0.669	1.419	0.581	0.480	0.0858
³¹ P	3.197	0.649	0.843	1.569	0.591	0.466	0.0786
³² S	3.244	0.587	0.765	1.553	0.582	0.457	0.0842
³⁵ Cl	3.351	0.640	0.902	1.696	0.587	0.441	0.0774
⁴⁰ Ar	3.553	0.724	0.644	1.527	0.592	0.438	0.0790
³⁹ K	3.496	0.629	0.902	1.782	0.582	0.418	0.0782
⁴⁰ Ca	3.534	0.576	0.789	1.723	0.575	0.414	0.0840
⁴⁵ Sc	3.710	0.676	0.868	1.836	0.583	0.396	0.0755
⁴⁸ Ti	3.829	0.667	0.673	1.681	0.580	0.401	0.0782
⁵¹ V	3.925	0.685	0.802	1.851	0.580	0.379	0.0732
⁵² Cr	3.945	0.656	0.703	1.779	0.576	0.381	0.0781
⁵⁵ Mn	4.008	0.712	0.802	1.928	0.581	0.362	0.0755
⁵⁶ Fe	4.031	0.680	0.714	1.860	0.577	0.364	0.0797
⁵⁹ Co	4.112	0.704	0.839	2.052	0.578	0.341	0.0755
⁵⁸ Ni	4.050	0.652	0.797	2.037	0.574	0.340	0.0827
⁶³ Cu	4.215	0.691	0.921	2.242	0.575	0.315	0.0744
⁶⁴ Zn	4.235	0.661	0.820	2.146	0.572	0.319	0.0782
⁷¹ Ga	4.438	0.746	0.812	2.174	0.577	0.310	0.0714
⁷⁴ Ge	4.542	0.713	0.687	2.027	0.572	0.320	0.0714
⁷⁵ As	4.543	0.711	0.867	2.337	0.572	0.287	0.0705
⁸⁰ Se	4.690	0.723	0.677	2.076	0.571	0.308	0.0697
⁷⁹ Br	4.631	0.696	0.905	2.484	0.570	0.268	0.0705
⁸¹ Br	4.696	0.714	0.831	2.362	0.570	0.277	0.0690
⁸⁷ Kr	4.694	0.969	0.657	2.108	0.593	0.300	0.0740
⁸² Rb	4.623	0.766	0.946	2.642	0.576	0.250	0.0746
⁸⁸ Sr	4.861	0.683	0.699	2.247	0.565	0.279	0.0702
⁸⁹ Y	4.868	0.672	0.856	2.568	0.564	0.247	0.0696
⁹⁰ Zr	4.877	0.658	0.788	2.481	0.563	0.253	0.0720
⁹³ Nb	4.877	0.766	0.927	2.786	0.572	0.226	0.0720

Nucleus	R	a_n	a_p	α_p	β_n	β_p	ρ_p
⁹⁸ Mo	5.006	0.774	0.728	2.438	0.571	0.251	0.0712
¹⁰² Ru	5.087	0.750	0.718	2.488	0.568	0.242	0.0715
¹⁰³ Rh	5.090	0.746	0.914	2.938	0.568	0.204	0.0707
¹⁰⁶ Pd	5.159	0.736	0.745	2.616	0.566	0.227	0.0716
¹⁰⁸ Pd	5.212	0.749	0.722	2.566	0.567	0.231	0.0698
¹⁰⁷ Ag	5.159	0.737	0.947	3.100	0.566	0.188	0.0709
¹¹⁴ Cd	5.327	0.757	0.711	2.610	0.566	0.223	0.0687
¹¹⁵ In	5.327	0.757	0.873	3.019	0.566	0.188	0.0684
¹¹⁶ Sn	5.340	0.736	0.748	2.766	0.564	0.206	0.0707
¹¹⁸ Sn	5.393	0.745	0.720	2.701	0.564	0.211	0.0691
¹²⁰ Sn	5.440	0.754	0.698	2.647	0.565	0.216	0.0675
¹²¹ Sb	5.447	0.749	0.948	3.284	0.564	0.167	0.0663
¹²⁶ Te	5.555	0.754	0.755	2.855	0.563	0.194	0.0657
¹²⁷ I	5.555	0.753	0.915	3.292	0.563	0.162	0.0656
¹³² Xe	5.657	0.761	0.754	2.926	0.563	0.186	0.0649
¹³³ Cs	5.658	0.759	0.923	3.401	0.563	0.152	0.0647
¹³⁸ Ba	5.751	0.776	0.759	3.012	0.563	0.176	0.0642
¹³⁹ La	5.755	0.768	0.911	3.459	0.562	0.146	0.0640
¹⁴⁰ Ce	5.766	0.751	0.798	3.193	0.561	0.161	0.0658
¹⁴¹ Pr	5.771	0.743	0.996	3.785	0.560	0.126	0.0653
¹⁴² Nd	5.780	0.726	0.848	3.410	0.559	0.145	0.0672
¹⁵² Sm	5.937	0.792	0.774	3.275	0.562	0.151	0.0650
¹⁵⁸ Gd	6.021	0.808	0.781	3.370	0.563	0.142	0.0644
¹⁶⁵ Ho	6.115	0.803	0.913	3.905	0.561	0.111	0.0637
¹⁶⁹ Tm	6.160	0.803	0.965	4.162	0.561	0.098	0.0641
¹⁸¹ Ta	6.318	0.827	0.935	4.244	0.561	0.091	0.0633
¹⁸⁴ W	6.354	0.836	0.821	3.888	0.562	0.105	0.0638
¹⁹⁵ Pt	6.444	0.921	0.827	4.071	0.566	0.095	0.0646
¹⁹⁷ Au	6.536	0.802	0.947	4.559	0.558	0.075	0.0623
²⁰² Hg	6.606	0.817	0.793	4.021	0.558	0.095	0.0619
²⁰⁵ Tl	6.638	0.828	0.899	4.465	0.559	0.077	0.0614
²⁰⁸ Pb	6.670	0.839	0.805	4.142	0.559	0.088	0.0617

Table 1: Parameters of the neutron and proton densities of Gambhir and Patil calculated with the method described in [3].

Nucleus	R	a_n	ρ_n	Nucleus	R	a_n	ρ_n
¹⁶ O	2.416	0.575	0.0992	⁸⁹ Y	4.621	0.672	0.1044
¹⁹ F	2.407	0.705	0.1136	⁹⁰ Zr	4.718	0.658	0.0990
²³ Na	2.564	0.646	0.1214	⁹³ Nb	4.680	0.766	0.1013
²⁴ Mg	2.917	0.560	0.0919	⁹⁸ Mo	4.948	0.774	0.0935
²⁷ Al	2.715	0.630	0.1237	¹¹⁴ Cd	5.324	0.757	0.0906
²⁸ Si	3.031	0.549	0.0975	¹¹⁵ In	5.014	0.757	0.1069
³¹ P	2.874	0.649	0.1205	¹¹⁶ Sn	5.290	0.736	0.0928
³² S	3.082	0.587	0.1042	¹¹⁸ Sn	5.367	0.745	0.0916
³⁵ Cl	3.115	0.640	0.1105	¹²⁰ Sn	5.360	0.754	0.0943
⁴⁰ Ar	3.573	0.724	0.0899	¹²¹ Sb	5.165	0.749	0.1047
³⁹ K	3.172	0.629	0.1177	¹³⁸ Ba	5.594	0.776	0.0976
⁴⁰ Ca	3.424	0.576	0.0988	¹³⁹ La	5.519	0.768	0.1015
⁴⁸ Ti	3.875	0.667	0.0880	¹⁴² Nd	5.672	0.726	0.0952
⁵¹ V	3.622	0.685	0.1126	¹⁵² Sm	5.956	0.792	0.0895
⁵² Cr	3.866	0.656	0.0958	¹⁵⁸ Gd	6.063	0.808	0.0886
⁵⁵ Mn	3.760	0.712	0.1078	¹⁶⁵ Ho	6.053	0.803	0.0929
⁵⁶ Fe	3.980	0.680	0.0939	¹⁸¹ Ta	6.431	0.827	0.0860
⁵⁹ Co	3.924	0.704	0.1029	¹⁸⁴ W	6.407	0.836	0.0883
⁵⁸ Ni	3.900	0.652	0.1007	¹⁹⁵ Pt	6.364	0.921	0.0936
⁶³ Cu	4.011	0.691	0.1037	¹⁹⁷ Au	6.215	0.802	0.1039
⁶⁴ Zn	4.147	0.661	0.0959	²⁰⁵ Tl	6.470	0.828	0.0970
⁷⁴ Ge	4.509	0.713	0.0924	²⁰⁸ Pb	6.550	0.839	0.0950
⁸⁸ Sr	4.707	0.683	0.0988				

Table 2: Parameters of the neutron densities of Gambhir and Patil calculated with the method described in [4].

1) of these quantities as function of A using (9) and (10): That is for each value of A we choose a particular combination of N and Z satisfying the relation $A = N+Z$.

Another possible application of $\langle r^2 \rangle$ and $\hbar\omega$ calculated with $\rho_{GP}(r)$ is to express more consistently the probability for recoilless Λ -production in nuclei $P(n_i, n_i)$ [10] (see also [11]). In the case in which only the outer shell neutrons are considered P is given by the expression :

$$P(n_i, n_i) = \bar{I}_{n_i}^2 \exp \left[\frac{-\hbar^2 q^2}{(\mu_\Lambda \hbar\omega_\Lambda + \mu_n \hbar\omega_n)} \left(\frac{2n_i}{3} + 1 \right) \right] \quad (14)$$

where $(2n+l) = n_i$, μ_Λ , μ_n are the reduced masses of the Λ -core and neutron-core systems and \bar{I}_{n_i} is the average overlap integral over all the neutron states of the outer shell with the oscillator quantum number n_i . Thus one can remove the approximation $\hbar\omega_n = \hbar\omega_p = \hbar\omega_N$ used in previous publications [10,11]. In addition the expressions for the m.s. radius and $\hbar\omega_n$ might be useful to calculate easily the point proton and point neutron form factor at low momentum transfer by means of Debye-Waller type expressions (see (2.2) and (2.8) of [12]) avoiding again the above approximation.

Nucleus	SF	GP	"Expt"	HF
^{16}O	2.60	2.74	2.62	2.69
^{24}Mg	3.01	3.02	2.95	
^{28}Si	3.08	3.13	3.02	
^{32}S	3.28	3.34	3.15	
^{40}Ca	3.41	3.54	3.38	3.43
^{56}Fe	3.77	3.75	3.70	3.54
^{58}Ni	3.77	3.85	3.67	3.58
^{64}Zn	4.01	3.99	3.86	
^{116}Sn	4.67	4.63	4.56	4.58
^{208}Pb	5.37	5.57	5.45	5.45

Table 3: Comparison of proton r.m.s. values $\langle r^2 \rangle_p^{1/2}$ of $\rho_{GP}(r)$ with values obtained from various approaches (for details see text).

A comparison of $\rho_{SF}(r)$ and $\rho_{GP}(r)$ can be made by tabulating the cor-

responding r.m.s radii for various nuclei. In table 3 we show proton rms radii $\langle r^2 \rangle_p^{1/2}$ for the density $\rho_{SF}(r)$ according to ref [2] and for the density $\rho_{GP}(r)$. In column 4 “experimental” values extracted from [13] are displayed and in column 5 the available Hartree-Fock(HF) results from [14] are shown as well. An advantage of $\rho_{GP}(r)$ is that the values predicted for $\langle r^2 \rangle_p$ compared with experimental values are very accurate throughout the periodic table.

Neutron rms radii calculated with $\rho_{GP}(r)$ can be compared with the radii for neutron distributions extracted from experimental shifts and widths of pionic atoms according to [15]. In column 2 of table 4 we present results for $\langle r^2 \rangle_n^{1/2}$ obtained in [15] using the phenomenological optical potential developed in [16-18] and in column 3 we show the average values of $\langle r^2 \rangle_n^{1/2}$ deduced in [15] from two different potentials widely used in the literature:

Nucleus	[15]	(mean)	HF	GP1	GP2
^{19}F	2.73	2.86	2.96	2.97	2.75
^{23}Na	2.93	3.00	2.96	3.01	2.76
^{24}Mg	3.07	3.12	3.06	2.89	2.86
^{27}Al	3.17	3.11	3.09	3.10	2.83
^{28}Si	3.11	3.21	3.06	2.99	2.91
^{32}S	3.13	3.31	3.20	3.15	3.01
^{40}Ar	3.63	3.54	3.52	3.59	3.56
^{40}Ca	3.52	3.52	3.56	3.32	3.22
^{56}Fe	3.89	3.89	3.84	3.83	3.76
^{63}Cu	3.96	3.99	3.99	3.97	3.80
^{75}As	4.22	4.20	4.19	4.22	4.20
^{195}Pt	5.55	5.56	5.61	5.85	5.77
^{197}Au	5.64	5.59	5.61	5.73	5.49
^{208}Pb	5.74	5.69	5.71	5.88	5.78

Table 4: Comparison of neutron-matter r.m.s. values, $\langle r^2 \rangle_n^{1/2}$, obtained using $\rho_{GP}(r)$, according to the method of [3] (GP1) and the method of [4] (GP2), with values coming from a study with pionic atoms [15] (second and third columns) and with HF results quoted in [15] (for more details see text).

The Seki and Masutani potential [19] and the potential of Meirav et al. [20]. In column 4 $\langle r^2 \rangle_n^{1/2}$ from Hartee-Fock calculations quoted in [15] are also shown, while in columns 5 and 6 we display results using the density $\rho_{GP}(r)$, derived first with the method described in [3] (GP1), where ρ_n is fixed equal to $0.090/fm^3$ and second with the method of ref. [4] (GP2). It is seen from tables 3 and 4 that the values of the r.m.s radii calculated with the simple method of Gambhir and Patil compare favorably with the values found in other more sophisticated studies.

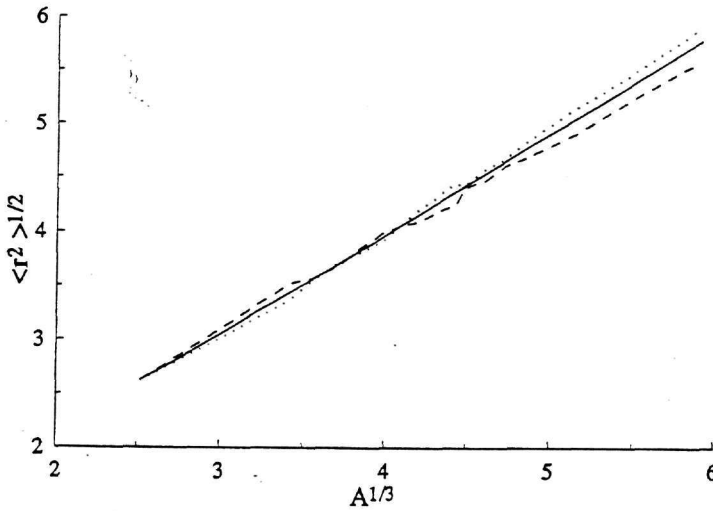
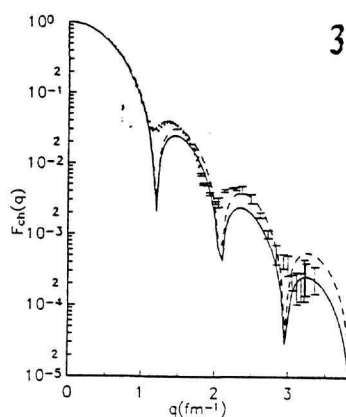
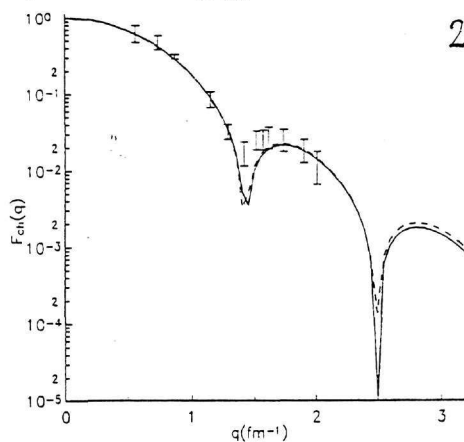


Figure 1 A schematic comparison of $\langle r^2 \rangle_m^{1/2}$ (solid line), $\langle r^2 \rangle_n^{1/2}$ (dotted line) and $\langle r^2 \rangle_p^{1/2}$ (dashed line), as functions of A , using equations (10) and (11) (see text).

Another comparison is to calculate the corresponding charge form factors in the Born approximation using both densities. The interesting point is that the parameters of ρ_{SF} are calculated by fitting an analytic expression for $F_{ch}(q)$ to the experimental values of $F_{ch}(q)$ coming from electron scattering,

while $\rho_{GP}(r)$ was found theoretically using as input the separation energies of the last particle and the calculation does not involve any fitting procedure. As an example, the charge form factors for ^{24}Mg and ^{40}Ca calculated with ρ_{GP} and ρ_{SF} are shown, together with experimental points, in figures 2 and 3 respectively. It is seen that the density $\rho_{GP}(r)$ gives a satisfactory $F_{ch}(q)$ compared with $F_{ch}(q)$ coming from $\rho_{SF}(r)$, though in the former calculation no fitting to the experimental $F_{ch}(q)$ is involved.



Figures 2,3. The charge form factors of ^{24}Mg and ^{40}Ca using the density $\rho_{GP}(r)$ (solid line) and with the density $\rho_{SF}(r)$ (dashed line). Experimental points and bars are shown as well.

It is noted that the central depression is not taken into account properly by $\rho_{GP}(r)$. However this density has a global character and may find use in cases where a global method is needed to provide simple analytic expressions

for various quantities which also give evidence of the dependence of these quantities on A , Z and N . This was the case with the applications discussed above and also in [3,4] where the authors used $\langle r^2 \rangle$ derived from $\rho_{GP}(r)$ in order to track the variation of $\hbar\omega$ as function of N , Z and A separately. It is also noted that although the results obtained using the density GP may not be completely satisfactory, this density has the attractive feature that for the determination of its parameters no fitting procedure is required. We conclude that the simple expressions for the densities $\rho_{GP}(r)$ may find ready use in various phenomenological nuclear studies.

4 Acknowledgments

One of the authors (G.A.L) would like to thank Professor M.E. Grypeos and the Department of Theoretical Physics of the Aristotle University of Thessaloniki for partial financial support.

References

- [1] Yu.N. Eldyshev, V.K. Lukyanov and Yu.S. Pol, Sov.J.Nucl. Phys. **16**,(1973) 282
- [2] V.V. Burov, Yu.V. Eldyshev, V.K. Lukyanov and Yu.S. Pol (1974) JINR preprint E4 8029, Dubna
- [3] Y.K. Gambhir and S.H.Patil,Z.Phys. A-Atoms and Nuclei **321**,(1985) 161
- [4] Y.K. Gambhir and S.H.Patil,Z.Phys. A-Atomic Nuclei **324**,(1986) 9
- [5] M.E. Grypeos, G.A. Lalazissis, S.E. Massen and C.P. Panos, J. Phys. G: Nucl. Part. Phys. **17** (1991) 1093
- [6] G.A. Lalazissis, M.E. Grypeos and S.E. Massen, J. Phys. G: Nucl. Part. Phys. **15** (1989) 303
- [7] G.A. Lalazissis, J. Phys. G: Nucl. Part. Phys. **19** (1993) 695

- [8] G.A. Lalazissis and C.P. Panos, *Z. Phys. A-Hadrons and Nuclei* **344**, (1992) 17
- [9] G.A. Lalazissis and C.P. Panos, *J.Phys.G.: Nucl. Part.Phys.* **19**, (1993) 283
- [10] M.E. Grypeos, G.A. Lalazissis, S.E. Massen and C.P. Panos, *J.Phys.G.: Nucl.Part.Phys.*, **16**, (1990) 1627
- [11] M.E. Grypeos, G.A. Lalazissis, S.E. Massen and C.P. Panos, *Z. Phys. A-Atomic Nuclei* **332** (1989) 391
- [12] M.E.Grypeos, G.A. Lalazissis, S.E.Massen and C.P.Panos, *Z. Naturforsch.* **47a** (1992) 1211
- [13] H. De Vries, C.W. De Jager and C. De Vries, *Atomic and Nuclear Data tables* **36** (1987) 495
- [14] R.C. Barrett and D.F. Jackson: *Nuclear sizes and structure* Oxford, Clarendon Press (1977)
- [15] C. Garcia-Recio, J.Nieves and E.Oset, *Nucl.Phys.* **A547** (1992) 473
- [16] C.Garcia-Recio, E.Oset and L.L. Salcedo, *Phys.Rev. C* **37** (1988) 194
- [17] C.Garcia-Recio, *Int. Workshop on pions in nuclei, Peniscola, 1991*, ed. E. Oset, M.Vicente-Vacas and C.Garcia-Recio (World Scientific, Singapore, 1992) p.320
- [18] J.Nieves, E.Oset and C.Garcia-Recio, *University of Valencia preprint* (1992), submitted to *Nucl.Phys. A*
- [19] R.Seki and K. Masutani, *Phys.Rev. C* **27** (1983) 2799
- [20] O.Meirav, E.Friedman, R.R. Johnson, R.Olszewski and P. Weber, *Phys.Rev. C* **40** (1989) 843